Chapter 3

FLUID MECHANICS

Fluid mechanics and thermodynamics are the fundamental sciences used for the aerodynamic design and analysis of axial-flow compressors. This chapter highlights some fundamental concepts from fluid mechanics to complement the concepts from thermodynamics covered in Chapter 2. The governing equations will be developed in forms suitable for the various aerodynamic analyses commonly employed for axial-flow compressors. Detailed solution procedures will be covered in subsequent chapters.

Several types of fluid dynamic analysis are useful for this purpose. The through-flow analysis is widely used in both design and performance analysis. This involves solving the governing equations in the hub-to-shroud plane at stations located between blade rows. The flow is normally considered to be axisymmetric at these locations, but still three-dimensional because of the existence of a tangential velocity component. Empirical models are employed to account for the fluid turning and losses that occur when the flow passes through the blade rows. A simplification of this analysis is the "pitch-line" or "mean-line" one-dimensional flow model, which ignores the hub-to-shroud variations. These were very common for many years, but are no longer particularly relevant to the problem. Computers are sufficiently powerful today that there is really no need to simplify the problem that much. The through flow in an axial-flow compressor is strongly influenced by viscous effects near the end walls. The primary influence from these end-wall boundary layers is commonly described as end-wall blockage. An inviscid through-flow analysis ignores the low momentum fluid in the boundary layers and will overestimate the mass flow that the passage can accommodate for a given flow field solution. To compensate the common practice is to impose a blockage factor to effectively reduce the passage area. This requires consideration of boundary layer analysis to estimate the appropriate blockage factors to be used. More fundamental internal flow analyses are often useful for specific components, particularly blade rows. These include two-dimensional flow analyses in either the blade-to-blade or hub-to-shroud direction, and quasi-three-dimensional flow analyses developed by combining and interacting these two-dimensional analyses. Again, wall boundary layer analysis is often used to evaluate viscous effects. Any of these analyses may be used in a design mode as well as an analysis mode. A design mode seeks to define the gas path geometry (end-wall contours and blades) to produce the desired flow field, while an analysis mode seeks to predict the flow field from specified geometry.

Viscous computational fluid dynamics (CFD) solutions are also in use for axial-flow compressors. These are typically three-dimensional flow analyses, which consider the effects of viscosity, thermal conductivity and turbulence. In most cases, commercial viscous CFD codes are used although some in-house codes are in use within the larger companies. Most design organizations cannot commit the dedicated effort required to develop these highly sophisticated codes, particularly since viscous CFD technology is changing so rapidly that any code developed will soon be obsolete unless its development continues as an ongoing activity. Consequently, viscous CFD is not covered in this book beyond recognizing it as an essential technology and pointing out some applications for which it can be effectively used to supplement conventional aerodynamic analysis techniques.

NOMENCLATURE

a = sound speed
b = stream sheet thickness
C = absolute velocity
E = entrainment function
$\vec{e}$ = unit vector
f = body force
H = total enthalpy
h = static enthalpy
I = rothalpy
m = meridional coordinate
$\dot{m}$ = mass flow rate
n = normal coordinate
P = pressure
r = radius
$\vec{r}$ = position vector in space
s = entropy
T = temperature
u = velocity in x direction
$\vec{V}$ = general vector
v = velocity in y direction
W = relative velocity
$\dot{w}$ = power
x = coordinate along a wall
y = coordinate normal to a wall
z = axial coordinate
δ = boundary layer thickness
δ^* = displacement thickness
θ = tangential coordinate and momentum thickness
κ = curvature
ν = force defect thickness
ρ = gas density
τ = torque and shear stress
ϕ = streamline slope with axis and a general function
ω = rotation speed

Subscripts

e = boundary layer edge condition
m = meridional component
n = normal component
r = radial component
t = total thermodynamic condition
w = parameter at a wall
1 = blade inlet parameter and meridional defect parameter
11 = meridional defect parameter
12 = tangential flux defect parameter
2 = blade exit parameter and tangential defect parameter
22 = tangential defect parameter
θ = tangential component

Superscripts

$'$ = a relative value in the rotating coordinate system

3.1 FLOW IN A ROTATING COORDINATE SYSTEM

The analysis of the flow in rotor blade rows is accomplished in a coordinate system, which rotates with the blade. The flow conditions in a rotating coordinate system are referred to as the relative conditions. If a blade row is rotating with an angular velocity, ω, the relative tangential velocity in a coordinate system rotating with the blade, W_θ, is related to the absolute tangential velocity, C_θ, by

$$W_\theta = C_\theta - \omega r \tag{3-1}$$

The axial and radial velocity components are independent of the rotation, i.e.,

$$W_z = C_z \tag{3-2}$$

$$W_r = C_r \tag{3-3}$$

It will be more convenient to work with the meridional velocity component, W_m, defined as

$$W_m = \sqrt{W_z^2 + W_r^2} = C_m \tag{3-4}$$

W_m is the velocity component lying in the meridional (constant θ) plane and in a stream surface. A stream surface is defined as a surface having no fluid velocity component normal to it and, therefore, no mass flow across it. Thus, the defining characteristic of a stream surface is that the mass flow rate between it and the hub contour surface is constant everywhere. The meridional coordinate, m, is measured along the stream surface and in a meridional plane, i.e.,

$$(dm)^2 = (dr)^2 + (dz)^2 \tag{3-5}$$

For axial-flow compressors, it is almost always reasonable to assume stream surfaces are axisymmetric. That assumption will be used throughout this book. Figure 3-1 illustrates a schematic of a stream surface and unit vectors for the meridional and polar coordinates. Normal to these unit vectors, and to the stream surface, is the third coordinate of interest, the normal coordinate, n, as shown in Fig. 3-2. It is convenient to develop the governing equations of fluid mechanics in this "natural" coordinate system (θ, m, n), where by definition

$$W_n = C_n = 0 \tag{3-6}$$

Now consider the flow through a thin stream sheet, i.e., a thin annular passage bounded by two stream surfaces. The torque, τ, acting on the fluid between meridional stations 1 and 2 is given by conservation of angular momentum.

$$\tau = \dot{m}(r_2 C_{\theta 2} - r_1 C_{\theta 1}) \tag{3-7}$$

This torque must balance the power input, i.e.,

$$\dot{w} = \omega\tau = \omega\dot{m}(r_2 C_{\theta 2} - r_1 C_{\theta 1}) \tag{3-8}$$

Combining Eq. (3-8) with Eq. (2-4) yields the well-known Euler turbine equation

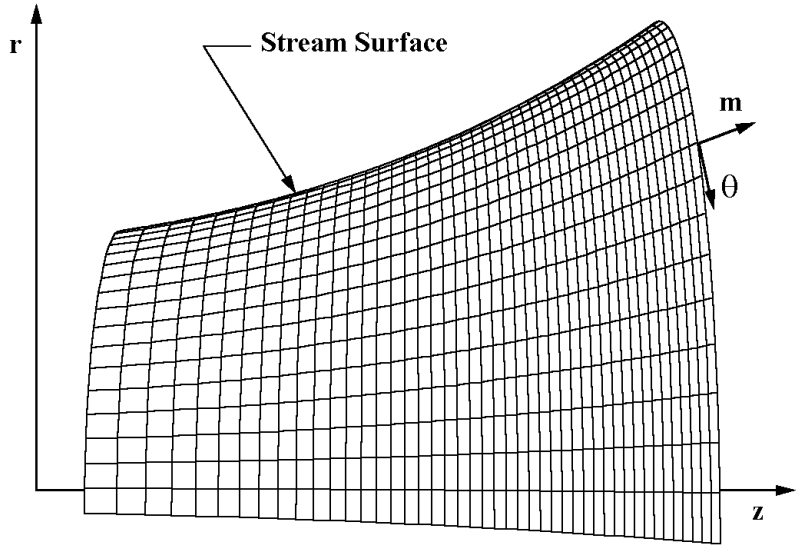

FIGURE 3-1 Schematic of a Stream Surface

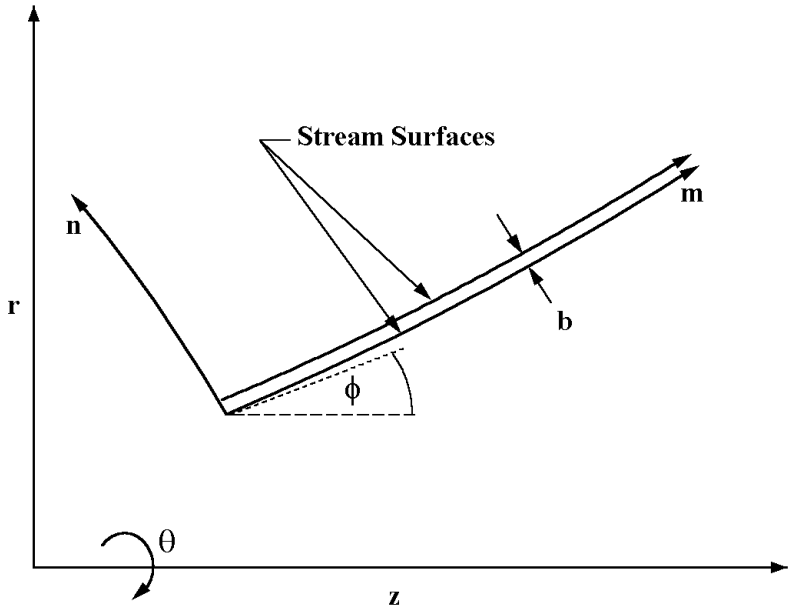

FIGURE 3-2 Natural Coordinate System

$$H_2 - H_1 = \omega(r_2 C_{\theta 2} - r_1 C_{\theta 1}) \tag{3-9}$$

This is the general energy equation relating the total enthalpy change produced by a transfer of mechanical energy between the fluid and a rotating blade row. It is convenient to introduce the rothalpy, I, defined by

$$I = H - \omega r C_\theta \tag{3-10}$$

On introducing Eq. (3-10) into Eq. (3-9), it can be seen that rothalpy is constant on a stream surface. Hence, rothalpy is the basic parameter expressing energy conservation for a rotating blade row. It is also valid for a stationary blade row, since $I = H$ in that case, and Eq. (3-9) requires that H be constant in the absence of energy transfer with a rotating blade row.

Aerodynamic analysis of axial-flow compressors involves alternately solving the governing equations in rotating coordinates (rotors) and stationary coordinates (stators). Hence, we need to relate the relative total enthalpy, H', in a rotating coordinate system to the absolute total enthalpy, H, in a stationary coordinate system. Noting that static thermodynamic conditions are identical for either coordinate system,

$$h = H' - \tfrac{1}{2} W^2 = H - \tfrac{1}{2} C^2 \tag{3-11}$$

The relative velocity, W, follows from Eqs. (3-1), (3-4) and (3-6)

$$W = \sqrt{W_m^2 + W_\theta^2} \tag{3-12}$$

Equations (3-1), (3-10), (3-11) and (3-12) combine to yield

$$H' = H - \omega r C_\theta + \tfrac{1}{2}(\omega r)^2 = I + \tfrac{1}{2}(\omega r)^2 \tag{3-13}$$

Noting that entropy is constant between total and static conditions, and therefore between a rotating and a stationary coordinate system, Eq. (3-13) can be used to relate the two coordinate systems. For example, the change in all other relative total thermodynamic conditions between the two coordinate systems can be calculated from an appropriate equation of state as a function of (H, H', s). This requires calculation of the isentropic change in the parameter of interest for a specified change in enthalpy. Hence, Eq. (3-13) is an important relation that allows us to relate all thermodynamic parameters between the stationary and the rotating coordinate systems. Also, since I is constant on the stream surface, Eq. (3-13) allows calculation of H' at all points on a stream surface when one value is known, e.g., at the inlet.

3.2 ADIABATIC INVISCID COMPRESSIBLE FLOW

Adiabatic compressible inviscid flow analysis is commonly used in turbomachinery. This flow model assumes that fluid viscosity and thermal conductivity can be neglected. Basic conservation of mass, momentum and energy, supported by a suitable equation of state, govern the flow. It is useful to derive the governing equations in a rotating coordinate system, noting that these equations will be valid for a stationary coordinate system if ω is set to zero. The vector form of the momentum equation can be written (Novak, 1967; Vavra, 1960; Wu, 1952)

$$\frac{d\vec{C}}{dt} = -\frac{1}{\rho}\vec{\nabla}P = \frac{d\vec{W}}{dt} + 2(\vec{\omega} \times \vec{W}) + \vec{\omega} \times (\vec{\omega} \times \vec{r}\,) \tag{3-14}$$

where the last two terms in Eq. (3-14) are the Coriolis and centrifugal accelerations imposed by the rotating coordinate system, and the time derivative is the substantial derivative, i.e.,

$$\frac{d\vec{W}}{dt} = \frac{\partial \vec{W}}{\partial t} + (\vec{W} \cdot \vec{\nabla})\vec{W} \tag{3-15}$$

Hence, the momentum equation in rotating coordinates is

$$\frac{\partial \vec{W}}{\partial t} + (\vec{W} \cdot \vec{\nabla})\vec{W} + 2(\vec{\omega} \times \vec{W}) + \vec{\omega} \times (\vec{\omega} \times \vec{r}\,) = -\frac{\vec{\nabla}P}{\rho} \tag{3-16}$$

Using standard vector identities, this equation can also be written as

$$\frac{\partial \vec{W}}{\partial t} - \vec{W} \times (\vec{\nabla} \times \vec{W} + 2\vec{\omega}) - r\omega^2 \vec{e}_r + \frac{1}{2}\vec{\nabla} W^2 = -\frac{\vec{\nabla} P}{\rho} \tag{3-17}$$

where $\vec{e}_r$ is a unit vector in the radial direction. On introducing Eqs. (2-3), (2-8), (3-10) and (3-11), an alternate form of Eq. (3-17) is obtained.

$$\frac{\partial \vec{W}}{\partial t} - \vec{W} \times (\vec{\nabla} \times \vec{W} + 2\vec{\omega}) = T\vec{\nabla} s - \vec{\nabla} I \tag{3-18}$$

The continuity and energy equations in vector form are

$$\frac{\partial \rho}{\partial t} + \vec{\nabla} \cdot (\rho \vec{W}) = 0 \tag{3-19}$$

$$\frac{\partial I}{\partial t} - \frac{1}{\rho}\frac{\partial P}{\partial t} + (\vec{W} \cdot \vec{\nabla}) I = 0 \tag{3-20}$$

Equations (3-16) through (3-20) are vector equations, which are valid in any coordinate system. To express the equations in the natural coordinates (θ, m, n), standard curvilinear coordinate transformations are used. These can be found in most advanced calculus books, which cover vector field theory. Vavra (1960, Appendix A) provides specific and detailed derivations of the vector operators and governing equations in natural coordinates. For general reference, the important vector operators are provided without derivation at the end of this chapter. The resulting governing equations are

$$\frac{\partial \rho}{\partial t} + \frac{1}{r}\left[\frac{\partial r\rho W_m}{\partial m} + \frac{\partial \rho W_\theta}{\partial \theta}\right] + \kappa_n \rho W_m = 0 \tag{3-21}$$

$$\frac{\partial W_m}{\partial t} + W_m \frac{\partial W_m}{\partial m} + \frac{W_\theta}{r}\frac{\partial W_m}{\partial \theta} - \frac{\sin\phi}{r}[W_\theta + \omega r]^2 = -\frac{1}{\rho}\frac{\partial P}{\partial m} \tag{3-22}$$

$$\frac{\partial W_\theta}{\partial t} + W_m \frac{\partial W_\theta}{\partial m} + \frac{W_\theta}{r}\frac{\partial W_\theta}{\partial \theta} + \frac{W_m \sin\phi}{r}[W_\theta + 2\omega r] = -\frac{1}{r\rho}\frac{\partial P}{\partial \theta} \tag{3-23}$$

$$\kappa_m W_m^2 + \frac{\cos\phi}{r}[W_\theta + \omega r]^2 = \frac{1}{\rho}\frac{\partial P}{\partial n} \tag{3-24}$$

$$\frac{\partial I}{\partial t} - \frac{1}{\rho}\frac{\partial P}{\partial t} + W_m \frac{\partial I}{\partial m} + \frac{W_\theta}{r}\frac{\partial I}{\partial \theta} = 0 \tag{3-25}$$

The curvature of the stream sheet, κ_m, and of the normal surface, κ_n, are related to the angle ϕ shown in Fig. 3-2.

$$\kappa_m = -\frac{\partial \phi}{\partial m} \tag{3-26}$$

$$\kappa_n = \frac{\partial \phi}{\partial n} = \frac{1}{b}\frac{\partial b}{\partial m} \tag{3-27}$$

Parameter b in Eq. (3-27) is the thickness of a stream sheet bounded by two stream surfaces, as shown in Fig. 3-2. Hence, the curvature κ_n is related to the meridional divergence or convergence of the stream surfaces. That form is useful in some applications of these governing equations, particularly when analyzing the two-dimensional flow in a blade-to-blade stream surface. Equations (3-22) through (3-24) can be expressed differently using Eq. (3-18).

$$\frac{\partial W_m}{\partial t} + \frac{W_\theta}{r}\left[\frac{\partial W_m}{\partial \theta} - \frac{\partial (rW_\theta + \omega r^2)}{\partial m}\right] = T\frac{\partial s}{\partial m} - \frac{\partial I}{\partial m} \tag{3-28}$$

$$\frac{\partial W_\theta}{\partial t} - \frac{W_m}{r}\left[\frac{\partial W_m}{\partial \theta} - \frac{\partial (rW_\theta + \omega r^2)}{\partial m}\right] = T\frac{\partial s}{\partial \theta} - \frac{\partial I}{\partial \theta} \tag{3-29}$$

$$\kappa_m W_m^2 + \frac{W_\theta}{r}\frac{\partial (rW_\theta + \omega r^2)}{\partial n} + W_m\frac{\partial W_m}{\partial n} = \frac{\partial I}{\partial n} - T\frac{\partial s}{\partial n} \tag{3-30}$$

Since there are only two velocity components (i.e., $W_n = 0$), one of the three momentum equations is redundant. The redundant equation has been replaced by the assumption that the stream surfaces are known or can somehow be determined as part of the solution. If the meridional surfaces are not stream surfaces, the governing equations must be modified to include a normal velocity component, W_n. This will not be required for analyses described in this book, although there is no reason why a flow analysis could not be accomplished in an arbitrary (θ, m, n) coordinate system. Aungier (2000) includes the more general form of the governing equations appropriate for that type of analysis.

3.3 ADIABATIC INVISCID COMPRESSIBLE FLOW APPLICATIONS

The governing equations are applied in a variety of analyses in the aerodynamic design and analysis of axial-flow compressors. Most analyses employ the time-steady form of the governing equations, although the unsteady form does find application when the fluid velocity exceeds the sonic flow velocity. One of the most common applications is to determine the flow in the meridional plane. This application normally restricts the solution to stations outside of the blade rows, using empirical models to impose the influence of blade rows between stations in terms of fluid turning and total pressure loss correlations. These analyses treat the flow as axisymmetric to require conservation of mass, normal momentum and energy. Early practice was to develop these analyses in a simple cylindrical coordinate system (θ, m, r) such that the normal coordinate is replaced by the radial coordinate. Hence, the normal momentum equation was commonly referred to as the radial equilibrium equation in that context. Various simplifications may be employed in these analyses. If stream surface curvature is neglected ($\kappa_m = 0$) and the gradient of entropy across the passage is assumed to be zero, the term "simple radial equilibrium" has been used to describe the analysis. If the gradient of entropy is included, the solution is often referred to as "simple non-isentropic

radial equilibrium." When curvature and entropy are both included, the term "full radial equilibrium" is often used. Advances in computer technology and numerical analysis techniques have reduced the role of simple radial equilibrium solutions to cases where the entropy gradient cannot be properly defined, such as the general-purpose stage design described in Chapter 10. Simple non-isentropic radial equilibrium continues to be useful in basic blade row or stage design, where the streamline curvatures to be encountered in the actual compressor are not known. Indeed, simple non-isentropic radial equilibrium analysis is often quite sufficient for actual axial-flow compressors, where stream surface curvatures may be negligible. This is often true for industrial axial-flow compressors. When the stream surface curvature can be ignored, a dramatic reduction in computation time is realized, since the analysis becomes a simple marching solution. This follows from the fact that the flow at any axial station is not dependent on the flow at downstream stations. A simple variant used by this writer is to approximate stream surface curvatures from end-wall contours by simple linear interpolation. This allows the advantages of a simple non-isentropic radial equilibrium analysis, yet can approximate curvatures imposed by end-wall contour design.

Solutions for the two-dimensional flow in the meridional plane within blade passages are also fairly common. These usually seek to predict the average flow in the passage from the hub to the shroud as a two-dimensional flow problem. In the more general case, these hub-to-shroud analyses may solve for the two-dimensional flow on specific stream surfaces from hub to shroud. In both cases, either the flow angle or W_θ distributions throughout the passage must be supplied to replace solution of the tangential momentum equation.

Analysis of the flow passing through a blade row and lying on a stream surface is also common in axial-flow compressor design and analysis. These two-dimensional flow analyses are commonly called blade-to-blade flow analyses. Typically, the stream surface geometry is specified along with the distribution of the stream sheet thickness, b. Then, conservation of mass, energy, tangential momentum and meridional momentum can describe the flow. If the flow is assumed to be isentropic, Eqs. (3-28) and (3-29) show that one of the momentum equations is redundant, resulting in a simpler problem. This is fairly common practice for subsonic flow problems and is referred to as potential flow or irrotational flow. This results in a classical boundary value problem of an elliptic equation. Indeed, the governing equations for inviscid flow are elliptic in form as long as $W < a$ throughout the flow field. When supersonic flow is encountered ($W > a$), the governing equations become hyperbolic in mathematical form, which requires a marching type solution—such as the method of characteristics—rather than a boundary value problem solution. Cases where the flow is supersonic throughout are rare. Usually mixed subsonic-supersonic flow is involved. Then the time-steady governing equations are elliptic in some regions and hyperbolic in others, requiring two different solution techniques that must be matched together in some fashion. It is now fairly common practice to employ the time-unsteady equations for these cases. The advantage of that approach is that the unsteady equations of motion are hyperbolic in form for both subsonic and supersonic flow. This allows a single numerical method to be used for the mixed subsonic-supersonic flow case. This approach is commonly called the "time-dependent" or "time-marching" method of solution.

Hub-to-shroud and blade-to-blade flow analyses may also be combined to form a "quasi-three-dimensional" flow analysis within blade passages. A hub-to-shroud analysis can supply the stream surface geometry and stream sheet thickness distribution required for a blade-to-blade flow analysis. Similarly, a blade-to-blade flow analysis can supply the distribution of flow angle or tangential velocity required for a hub-to-shroud flow analysis. Thus an iterative solution solving these two two-dimensional flow problems with interaction between them can provide an approximate three-dimensional flow analysis. This approach was originally suggested by Wu (1952) and is a commonly used analysis technique.

Analysis of the complete three-dimensional inviscid flow problem is seldom used today. The additional information supplied relative to the simpler and faster quasi-three-dimensional flow analysis is relatively minor. Also, the evolution of three-dimensional viscous CFD analysis techniques has discouraged use of a three-dimensional inviscid flow analysis. As discussed at the beginning of this chapter, most turbomachinery design groups use one of the many excellent commercially available viscous CFD codes when a more detailed and fundamental analysis is needed.

3.4 BOUNDARY LAYER ANALYSIS

Adiabatic inviscid flow analyses, such as those described in the previous sections, are commonly augmented by boundary layer analysis techniques to evaluate viscous effects that are not considered by those analyses. The basic premise of boundary layer theory is that viscous effects are confined to a thin layer close to the physical surfaces bounding the flow passages (Schlichting, 1968, 1979). This is by no means always the case in axial-flow compressors, but selective use of boundary layer analysis has been found to be very effective in many applications. As with the discussion of three-dimensional inviscid flow analysis in the previous section, practical trade-offs with fully viscous flow analyses must be considered. Boundary layers in axial-flow compressors always involve significant three-dimensional character. Yet, there is little merit to a fully three-dimensional boundary layer analysis today, when commercially available viscous CFD codes can treat the problem much more accurately. Rather, it is the simplified boundary layer analysis techniques that are most effective in augmenting the inviscid flow analyses discussed in the previous section. Indeed, it is little short of remarkable that boundary layer analysis has been used so effectively in axial-flow compressor design and analysis, considering the fact that the fundamental boundary layer approximations are almost always violated to some degree and very often to a substantial degree. There are two important types of boundary layer analysis commonly used in axial-flow compressor aerodynamics. These involve boundary layers on the blade surfaces and those on the compressor end-wall contours. Blade surface boundary layers are of interest since they play a key role in viscous losses and stall or boundary layer separation. End-wall boundary layers are extremely important in performance analysis, since they can produce substantial viscous blockage effects that have significant impact on a compressor's performance.

Two-dimensional boundary layer analysis is a useful approximation for blade surface boundary layers, particularly in blade design. The primary goals of blade design are really governed by viscous effects, namely minimizing viscous losses and avoiding or delaying flow separation. Two-dimensional boundary layer analysis provides at least a qualitative assessment of these effects, yet adds very little complexity or computational time to the overall analysis. Indeed, conventional practice for blade design is to design blade sections in the context of simple two-dimensional cascades, where two-dimensional boundary layer analysis is directly applicable. These blade sections are then "stacked" to create the actual three-dimensional compressor blade. When applied to the actual compressor blade surface boundary layers, two-dimensional boundary layer analysis provides only qualitative results, since three-dimensional effects that are not considered by the analysis often become significant.

By contrast, end-wall boundary layers are necessarily three-dimensional, due to the presence of the swirl velocity component and tangential blade forces. Similar to inviscid flow analysis in the meridional plane, it is fairly common practice to conduct the boundary layer analysis for stations between blades—where an axisymmetric, three-dimensional boundary layer approximation can be used—while relying on empirical models to impose the blade row influence. This approach is a common basis for end-wall boundary layer blockage calculations for aerodynamic performance analysis (e.g., Balsa and Mellor, 1975). This axisymmetric three-dimensional boundary layer model has also been used within blade passages to provide an approximation to the boundary layer averaged between blade passages (Horlock, 1970, Aungier, 2000). Again, empirical models are required to model the influence of blade forces.

The basic boundary layer equations relevant to these two types of boundary layers will be developed in the remainder of this chapter. Specific applications of these governing equations will be discussed, as required, in subsequent chapters to support the various inviscid flow analyses.

3.5 TWO-DIMENSIONAL BOUNDARY LAYER ANALYSIS

Basic conservation of mass and momentum provide the governing equations for two-dimensional boundary layer flow over an adiabatic wall.

$$\frac{\partial \rho b u}{\partial x} + \frac{\partial \rho b v}{\partial y} = 0 \tag{3-31}$$

$$u\frac{\partial u}{\partial x} + v\frac{\partial u}{\partial y} + \frac{1}{\rho}\frac{\partial P}{\partial x} = \frac{1}{\rho}\frac{\partial \tau}{\partial y} \tag{3-32}$$

where τ is the shear stress. The coordinates (x, y) and velocity components (u, v) are illustrated in Fig. 3-3, along with a typical boundary layer velocity profile. The stream sheet thickness, b, has been included in Eq. (3-31) since it is often a function of x in turbomachinery applications, i.e., streamlines often converge or diverge. This directly affects conservation of mass. The basic assumption of boundary layer theory is that the pressure is constant across the

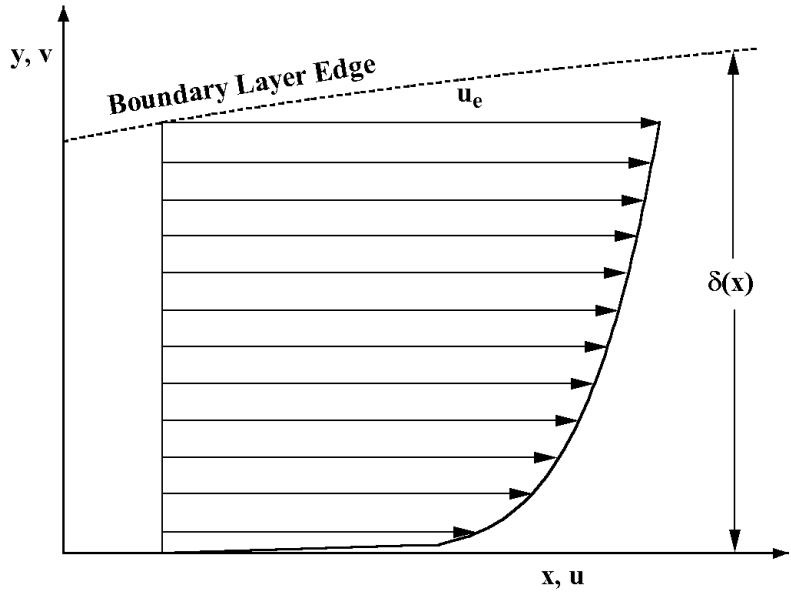

FIGURE 3-3 Boundary Layer Nomenclature

boundary layer, i.e., P is a function of x only. Boundary layer analysis in turbomachinery is most conveniently accomplished by applying the governing equations in integral form. Equation (3-31) can be integrated across the boundary layer, using the Liebnitz rule to interchange the order of integration and differentiation, to yield

$$\frac{\partial}{\partial x}\int_0^{\delta} b\rho u dy = b\rho_e u_e \frac{\partial \delta}{\partial x} - b\rho_e v_e = \frac{\partial}{\partial x}[b\rho_e u_e(\delta - \delta^*)] \tag{3-33}$$

The subscript e denotes inviscid flow conditions at the boundary layer edge, δ is the boundary layer thickness and δ^* is called the displacement thickness or mass defect thickness, defined as

$$\rho_e u_e \delta^* = \int_0^{\delta} [\rho_e u_e - \rho u] dy \tag{3-34}$$

Equation (3-34) can be rewritten as

$$\int_0^{\delta} \rho u dy = \rho_e u_e [\delta - \delta^*] \tag{3-35}$$

The displacement thickness is a fictitious thickness that can be used to correct the mass balance relative to the inviscid flow solution. As seen from Eq. (3-35), if the inviscid boundary layer edge or "free stream" conditions are applied within the boundary layer and the thickness δ^* is assumed to have zero mass flow, mass conservation will be corrected for viscous effects. Equations (3-31) and (3-32) can be combined to express the momentum equation in conservation form. This yields

$$\frac{1}{b}\frac{\partial b\rho u^2}{\partial x}+\frac{\partial \rho uv}{\partial y}+\frac{\partial P}{\partial x}=\frac{\partial \tau}{\partial y} \tag{3-36}$$

Analogous to the displacement thickness, the momentum thickness or momentum defect thickness is defined as

$$\rho_e u_e^2\theta=\int \rho u[u_e-u]dy \tag{3-37}$$

Equations (3-35) and (3-37) combine to yield

$$\int_0^{\delta}\rho u^2dy=\rho_e u_e^2[\delta-\delta^*-\theta] \tag{3-38}$$

If the free stream conditions are applied within the boundary layer with no flow in the thickness δ^* and, in addition, no momentum in the thickness θ, momentum conservation will be corrected for viscous effects. Hence, if $\delta^*$and θ can be predicted, we have a simple method to correct the known inviscid free stream mass and momentum flux for viscous effects. This is really the basis of integral boundary layer analysis methods. Integrating Eq. (3-36) across the boundary layer, again using the Liebnitz rule, and noting that $P = P_e$ is constant across the boundary layer, yields

$$\frac{\partial}{\partial x}\int_0^{\delta} b\rho u^2dy-\rho_e u_e^2\frac{\partial \delta}{\partial x}+\rho_e u_e v_e+\delta\frac{\partial P_e}{\partial x}=-\tau_w \tag{3-39}$$

Combining Eqs. (3-33), (3-38) and (3-39) yields

$$\frac{1}{b}\frac{\partial}{\partial x}[b\rho_e u_e^2(\delta-\delta^*-\theta)]-\frac{u_e}{b}\frac{\partial}{\partial x}[b\rho_e u_e(\delta-\delta^*)]+\delta\frac{\partial P_e}{\partial x}=-\tau_w \tag{3-40}$$

Equation (3-40) can be rearranged to yield

$$\frac{1}{b}\frac{\partial b\rho_e u_e^2\theta}{\partial x}+\delta^*\rho_e u_e\frac{\partial u_e}{\partial x}-\tau_w=\delta\left[\frac{\partial P_e}{\partial x}+\rho_e u_e\frac{\partial u_e}{\partial x}\right] \tag{3-41}$$

By applying Eq. (3-32) at the boundary layer edge, where the gradients of u and τ in the y direction are zero, it is easily seen that the right-hand side of Eq. (3-41) is

identically zero. Hence, Eq. (3-41) reduces to the well-known momentum integral equation.

$$\frac{1}{b}\frac{\partial b\rho_e u_e^2\theta}{\partial x}+\delta^*\rho_e u_e\frac{\partial u_e}{\partial x}=\tau_w \tag{3-42}$$

In the special case of two-dimensional, axisymmetric flow, it can be noted that b is proportional to radius, r, and the momentum integral equation becomes

$$\frac{1}{r}\frac{\partial r\rho_e u_e^2\theta}{\partial x}+\delta^*\rho_e u_e\frac{\partial u_e}{\partial x}=\tau_w \tag{3-43}$$

The momentum integral equation is valid for both laminar and turbulent boundary layers. Laminar boundary layer analysis usually employs specific boundary layer flow profile assumptions to permit direct integration of the momentum integral equation. Turbulent boundary layer analysis usually employs several empirical models for solution, which may include specific boundary layer flow profile assumptions. Usually, turbulent boundary layer analysis employs a second conservation equation, such as conservation of mass, energy or moment of momentum (Rotta, 1966). This writer prefers conservation of mass as the second equation, commonly called the entrainment equation. In this case, Eq. (3-33) is written in the form

$$\frac{\partial}{\partial x}[b\rho_e u_e(\delta-\delta^*)]=b\rho_e u_e E \tag{3-44}$$

The parameter E is called the entrainment function, which specifies the rate at which free stream fluid is entrained into the boundary layer at the boundary layer edge. To employ this model, an empirical correlation for E is required, which must be derived from experiment. Combining Eqs. (3-33) and (3-44), it is seen that the entrainment function is given by

$$E=\frac{\partial\delta}{\partial x}-\frac{v_e}{u_e} \tag{3-45}$$

Indeed, entrainment is governed by the gradient of the shear stress at the boundary layer edge. Hence, entrainment should depend on the shape of the boundary layer profiles, which is the usual basis for empirical models.

3.6 AXISYMMETRIC THREE-DIMENSIONAL BOUNDARY LAYER ANALYSIS

Equation (3-43) describes axisymmetric boundary layers where the flow field is two-dimensional, i.e., there is no tangential velocity component. When a

tangential velocity component is present in an otherwise axisymmetric flow field, the meridional and tangential components of the boundary layer profiles develop differently, resulting in a three-dimensional flow problem. The analysis of these problems is referred to as axisymmetric three-dimensional boundary layer analysis. This type of analysis is directly applicable to swirling flows in annular passages with no blades or vanes present, such as inlets and diffusers [e.g., Aungier 1988(b); Davis, 1976; Senoo et al., 1977]. This model has also been used effectively in axial-flow compressor performance analysis with application to stations between blade rows (e.g., Balsa and Mellor, 1975). When a blade row lies between successive computing stations, the axisymmetric assumption will have been violated within the blade passage. This requires use of empirical models to address the influence of the blade rows. Horlock (1970) also reports some success while applying this model within blade row passages. While these flows are far from axisymmetric, this model is used to provide an evaluation of the average or mean boundary layer behavior between the blades on the end-wall contours. Aungier (2000) uses this approach for quasi-three-dimensional flow analysis, a practice also followed in this book.

The governing equations for axisymmetric three-dimensional boundary layer flow in a rotating coordinate system in natural coordinates (θ, m, y) are

$$\frac{1}{r}\frac{\partial \rho W_m}{\partial m} + \frac{\partial \rho W_y}{\partial y} = 0 \tag{3-46}$$

$$W_m \frac{\partial W_m}{\partial m} + W_y \frac{\partial W_m}{\partial y} - \frac{\sin\phi}{r}(W_\theta + \omega r)^2 = \frac{1}{\rho}\left[f_m - \frac{\partial P_e}{\partial m} - \frac{\partial \tau_m}{\partial y} \right] \tag{3-47}$$

$$W_m \frac{\partial W_\theta}{\partial m} + W_y \frac{\partial W_\theta}{\partial y} + \frac{\sin\phi}{r} W_m (W_\theta + 2\omega r) = \frac{1}{\rho}\left[f_\theta - \frac{\partial \tau_\theta}{\partial y} \right] \tag{3-48}$$

A rotating coordinate system is needed for turbomachinery applications, since end-walls may be either rotating or stationary. The coordinate system should rotate with the end-wall to simplify imposing the boundary condition that all velocity components are identically zero at the wall. The terms f_m and f_θ in Eqs. (3-47) and (3-48) are body force terms used to account for blade forces acting on the flow. The blade forces at the boundary layer edge can be evaluated directly by applying Eqs. (3-47) and (3-48) to the inviscid flow at the boundary layer edge, where all inviscid free stream conditions are known and where W_n and the shear stress terms are identically zero. Hence,

$$f_{me} = \rho_e W_{me} \frac{\partial W_{me}}{\partial m} + \frac{\partial P_e}{\partial m} - \frac{\sin\phi}{r}\rho_e (W_{\theta e} + \omega r)^2 \tag{3-49}$$

$$f_{\theta e} = \rho_e W_{me} \frac{\partial W_{\theta e}}{\partial m} + \frac{\sin\phi}{r}\rho_e W_{me}(W_{\theta e} + 2\omega r) = \frac{\rho_e W_{me}}{r}\frac{\partial r C_{\theta e}}{\partial m} \tag{3-50}$$

The boundary layer equations are converted to integral form in the same fashion as described earlier. The algebra is more tedious and several additional defect thicknesses are required. The resulting integral equations are

$$\frac{\partial}{\partial m}[r\rho_e W_{me}(\delta - \delta_1^*)] = r\rho_e W_e E \tag{3-51}$$

$$\frac{\partial}{\partial m}[r\rho_e W_{me}^2\theta_{11}] + \delta_1^* r\rho_e W_{me}\frac{\partial W_{me}}{\partial m} - \rho_e W_{\theta e}\sin\phi[W_{\theta e}(\delta_2^* + \theta_{22}) + 2\omega r\delta_2^*] = r[\tau_{mw} + f_{me}v_m] \tag{3-52}$$

$$\frac{\partial}{\partial m}[r^2\rho_e W_{me}W_{\theta e}\theta_{12}] + r\delta_1^*\rho_e W_{me}\left[r\frac{\partial W_{\theta e}}{\partial m} + \sin\phi(W_{\theta e} + 2r\omega)\right] = r^2[\tau_{\theta w} + f_{\theta e}v_\theta] \tag{3-53}$$

The various mass, momentum and force defects used in these equations are defined as

$$\rho_e W_{me}\delta_1^* = \int_0^\delta (\rho_e W_{me} - \rho W_m)dy \tag{3-54}$$

$$\rho_e W_{me}^2\theta_{11} = \int_0^\delta \rho W_m(W_{me} - W_m)dy \tag{3-55}$$

$$\rho_e W_{me}W_{\theta e}\theta_{12} = \int_0^\delta \rho W_m(W_{\theta e} - W_\theta)dy \tag{3-56}$$

$$\rho_e W_{\theta e}\delta_2^* = \int_0^\delta (\rho_e W_{\theta e} - \rho W_\theta)dy \tag{3-57}$$

$$\rho_e W_{\theta e}^2\theta_{22} = \int_0^\delta \rho W_\theta(W_{\theta e} - W_\theta)dy \tag{3-58}$$

$$v_m f_{me} = \int_0^\delta (f_{me} - f_m)dy \tag{3-59}$$

$$v_\theta f_{\theta e} = \int_0^\delta (f_{\theta e} - f_\theta)dy \tag{3-60}$$

The momentum integral equations can be simplified by assuming that the blade forces are constant through the boundary layer. This would certainly be consistent with the usual boundary layer approximations, but it is now accepted that this is often not true for end-wall boundary layers of axial-flow compressors. Mellor and Wood (1971) advanced compelling arguments for the existence of force defects. Smith (1970) and Hunter and Cumpsty (1982) measured force defects experimentally. For vaneless annular passages, these body force terms will normally vanish, but they can be used to advantage when boundary layers merge to form fully developed viscous flow profiles [Aungier, 1988(b)].

3.7 Vector Operators in Natural Coordinates

The development of the governing equations in an axisymmetric natural coordinate system presented in this chapter requires use of several standard vector operators. Appendix A of Vavra (1960) provides detailed derivations of these operators. Here, the various operators are presented for reference purposes, without derivation. The gradient of any function ϕ is given by

$$\vec{\nabla}\phi = \frac{\partial \phi}{\partial m}\vec{e}_m + \frac{\partial \phi}{\partial n}\vec{e}_n + \frac{1}{r}\frac{\partial \phi}{\partial \theta}\vec{e}_\theta \tag{3-61}$$

where $\vec{e}$ is a unit vector. The divergence of any vector $\vec{V}$ is given by

$$\nabla \cdot \vec{V} = \frac{1}{r}\left[\frac{\partial r V_m}{\partial m} + \frac{\partial r V_n}{\partial n} + \frac{\partial V_\theta}{\partial \theta}\right] + \kappa_n V_m + \kappa_m V_n \tag{3-62}$$

The curl of any vector $\vec{V}$ is given by

$$\begin{aligned}\vec{\nabla} \times \vec{V} &= \left[\frac{\partial V_n}{\partial m} - \frac{\partial V_m}{\partial n} + \kappa_n V_n - \kappa_m V_m\right]\vec{e}_\theta \\ &+ \frac{1}{r}\left[\frac{\partial r V_\theta}{\partial n} - \frac{\partial V_n}{\partial \theta}\right]\vec{e}_m + \frac{1}{r}\left[\frac{\partial V_m}{\partial \theta} - \frac{\partial r V_\theta}{\partial m}\right]\vec{e}_n\end{aligned} \tag{3-63}$$

The Laplacian of any function ϕ is given by

$$\nabla^2\phi = \frac{1}{r^2}\frac{\partial^2 \phi}{\partial \theta^2} + \frac{\partial^2 \phi}{\partial m^2} + \frac{\partial^2 \phi}{\partial n^2} + \left[\frac{1}{r}\frac{\partial r}{\partial m} + \kappa_n\right]\frac{\partial \phi}{\partial m} + \left[\frac{1}{r}\frac{\partial r}{\partial n} + \kappa_m\right]\frac{\partial \phi}{\partial n} \tag{3-64}$$

In evaluating the convective derivative in Eq (3-15), the following vector identity is useful.

$$(\vec{V} \cdot \vec{\nabla})\vec{V} = \tfrac{1}{2}\vec{\nabla}(\vec{V} \cdot \vec{V}) - \vec{V} \times (\vec{\nabla} \times \vec{V}) \tag{3-65}$$

Equation (3-65) is usually written as

$$(\vec{V} \cdot \vec{\nabla})\vec{V} = \tfrac{1}{2}\vec{\nabla}V^2 - \vec{V} \times (\vec{\nabla} \times \vec{V}) \tag{3-66}$$

where V is the magnitude of the vector $\vec{V}$ as given by the dot product.

EXERCISES

3.1 Consider time-steady flow in a rotating coordinate system. Use Eqs. (3-28) through (3-30) to analyze the flow at stations outside of the

blade row passages where the flow can be considered to be axisymmetric, but may have a tangential velocity component. Develop equations governing the variation of C_θ, s and I on stream surfaces.

3.2 For the flow analysis in Exercise 3.1, modify Eq. (3-30) to consider cases where the relative flow angle, β', is known for all stream surfaces, where $\tan\beta' = W_\theta / W_m$. Repeat for cases where the absolute flow angle, β, is known for all stream surfaces where $\tan\beta = C_\theta / C_m$.

3.3 For Eq. (3-66), express V in terms of its components in the three coordinate directions. Derive an equation for $\frac{1}{2}\vec{\nabla}V^2$ in terms of V and its derivatives.

3.4 Consider one-dimensional, time-steady flow in a simple annular passage, i.e., $\kappa_m = 0$ and all gradients with respect to n and θ are identically zero. The passage width, $b(m)$, is a function of the meridional coordinate. Derive a set of governing equations for this problem from Eqs. (3-21) through (3-27).

3.5 Consider time-steady one-dimensional flow at the exit of a simple annular passage, with two identical boundary layers on the end-walls. The boundary layer parameters θ, δ^* and δ and the inviscid core flow data ρ, u and P at the passage exit are known. The flow is incompressible, i.e., ρ is constant and $P_t = P + {}^1/_2\rho u^2$. Develop expressions for the exit mass and momentum flow in terms of the boundary layer and inviscid core flow parameters.

3.6 Assume that the boundary layer flow and inviscid core flow in Exercise 3.5 mix instantaneously into a uniform flow with no change in static pressure. By requiring conservation of mass and momentum, show that the total pressure loss between the inviscid core flow and the fully mixed flow is given by

$$\Delta P_t = \frac{1}{2}\rho_e u_e^2[(2\delta^* / b)^2 + 4\theta / b]$$